



## Full Length Article

Hierarchical NiCo<sub>2</sub>O<sub>4</sub>@Co-Fe LDH core-shell nanowire arrays for high-performance supercapacitorWenQiang Chen<sup>a</sup>, Jiao Wang<sup>a</sup>, K.Y. Ma<sup>a</sup>, M. Li<sup>a,b</sup>, S.H. Guo<sup>a,c</sup>, F. Liu<sup>a</sup>, J.P. Cheng<sup>a,\*</sup><sup>a</sup>State Key Laboratory of Silicon Materials, Key Laboratory of Advanced Materials and Applications for Batteries of Zhejiang Province, School of Materials Science and Engineering, Zhejiang University, Hangzhou 310027, China<sup>b</sup>Research Institute of Narada Power Source Co., Ltd, Hangzhou 311305, China<sup>c</sup>Center for High Pressure Science and Technology Advanced Research (HPSTAR), Shanghai 201203, China

## ARTICLE INFO

## Article history:

Received 8 January 2018

Revised 7 April 2018

Accepted 27 April 2018

Available online 30 April 2018

## Keywords:

Core-shell structure

NiCo<sub>2</sub>O<sub>4</sub>@Co-Fe LDH

Nanowire arrays

Hybrid supercapacitor

## ABSTRACT

In this work, hierarchical NiCo<sub>2</sub>O<sub>4</sub>@Co-Fe layered double hydroxide (LDH) core-shell nanowire arrays on Ni foam were synthesized by facile hydrothermal and calcination methods. The pre-formed NiCo<sub>2</sub>O<sub>4</sub> nanowires on Ni foam acted as a substrate and then guided the deposition of Co-Fe LDH nanoflakes on their surface to form a highly porous hierarchical core-shell heterostructure. Meanwhile, NiCo<sub>2</sub>O<sub>4</sub> nanowires and Co-Fe LDH nanoflake films were also deposited on Ni foam. The materials were well characterized and used for electrochemical energy storage. The unique core-shell configuration of NiCo<sub>2</sub>O<sub>4</sub>@Co-Fe LDH can make full use of the synergistic effects of two components, provide sufficient electroactive sites as well as facilitate the charge transportation process. The as-prepared NiCo<sub>2</sub>O<sub>4</sub>@Co-Fe LDH nanowire arrays displayed outstanding electrochemical performances with a high specific capacitance of 1557.5 F g<sup>-1</sup> at 1 A g<sup>-1</sup>. The assembled two-electrode hybrid device NiCo<sub>2</sub>O<sub>4</sub>@Co-Fe LDH//activated carbon could deliver an energy density of 28.94 Wh kg<sup>-1</sup> at the power density of 950 W kg<sup>-1</sup>, showing a promising potential in energy storage and conversion.

© 2018 Elsevier B.V. All rights reserved.

## 1. Introduction

With increasing serious environmental pollution and fossil fuel consumption, the development of renewable energy storage devices becomes more and more important [1–4]. Supercapacitors, also called electrochemical capacitors, have attracted widespread attention from both industry and academia due to their high power density, superior rate capability, rapid charge/discharge process and long cycle life (>100 000 cycles) [5,6]. The performances of supercapacitor are essentially determined by the properties of electrode materials [7,8]. Recently, transition metal oxides and hydroxides have been extensively investigated as battery-type electrode materials for supercapacitor because of their high theoretical specific capacitance and abundant sources [9,10]. However, due to the intrinsic poor electrical conductivity and the short diffusion distance of electrolytes into the materials, the total capacitance can only be effectively contributed by the surface part of electroactive materials whereas the underneath parts can hardly participate in the charge storage process, which thus leading to an unsatisfactory electrochemical performance [11,12]. Therefore,

it is imperative to design electrode materials with advanced architectures for high conductivity and short ion diffusion distance.

In recent years, one-dimensional (1D) core-shell heteronanostructures have been considered as one of the most potential candidates for the next generation electrode design, since they can shorten the ion diffusion distance, increase the electrolyte-electrode contact area and enhance the structural stability [13–15]. Heterogeneous structures made of different core-shell battery-type materials are designed frequently, because both core and shell materials have Faradaic reactions during the charge/discharge processes, which will lead to a high specific capacitance [16]. To date, many transition metal oxide nanowires such as Fe<sub>2</sub>O<sub>3</sub> [17], Co<sub>3</sub>O<sub>4</sub> [18,19], CoO [20], ZnO [21], CuO [22] and NiO [23] etc. have been used as the core skeleton to support guest shell materials. Compared with other metal oxides, ternary nickel cobaltite (NiCo<sub>2</sub>O<sub>4</sub>) has aroused particular interest owing to its high electrical conductivity and superior stable electrochemical activity [24,25]. Recently, the reported core-shell 1D structures using NiCo<sub>2</sub>O<sub>4</sub> as core have displayed excellent electrochemical performances [26,27]. Yu and co-workers successfully fabricated NiCo<sub>2</sub>O<sub>4</sub>@MnO<sub>2</sub> core-shell nanowire arrays on carbon fiber paper, which demonstrated a high areal capacitance of 3.31 F cm<sup>-2</sup> at 2 mA cm<sup>-2</sup> and had only 12% capacitance loss after 2000 cycles at

\* Corresponding author.

E-mail address: [chengjp@zju.edu.cn](mailto:chengjp@zju.edu.cn) (J.P. Cheng).

10 mA cm<sup>-2</sup> [26]. Chen et al. synthesized NiCo<sub>2</sub>O<sub>4</sub>@NiWO<sub>4</sub> core-shell nanowire arrays on Ni foam, and the optimized electrode displayed remarkable electrochemical performance with a high specific capacitance of 1384 F g<sup>-1</sup> at 1 A g<sup>-1</sup> and superior cycling stability of 87.6% retention after 6000 cycles at 5 A g<sup>-1</sup> [27].

As a kind of two-dimensional (2D) materials, transition metal layered double hydroxides (LDH) exhibit a special layered structure. Their high surface area and fast ion transfer rates facilitate their applications in energy conversion and storage [28–31]. However, the aggregation and low electrical conductivity of LDHs restrict the ions/electrons transportation, which results in unsatisfactory electrochemical performances [32,33]. Therefore, thin LDH nanoflakes are often designed as the shell materials of 1D core-shell structure to increase their surface area and provide abundant electrolyte diffusion channels. X. He prepared NiCo<sub>2</sub>O<sub>4</sub>@NiCoAl-LDH core/shell nanoforest arrays as an electrode material, and the as-prepared composite showed a high specific capacitance (1814.2 F g<sup>-1</sup> at 1 A g<sup>-1</sup>) and outstanding cycling stability (93% retention after 2000 cycles at 10 A g<sup>-1</sup>) [34]. Co-Fe LDH with the co-existence of Co and Fe ions in the host layers has come into focus, which can be ascribed to the rich redox reactions and the synergistic effects during the electrochemical processes [35]. However, its low electrical conductivity and severe aggregation also limited its property, thus pure Co-Fe LDH usually exhibited low electrochemical performances. Co-Fe LDH nanoflakes have been also reported as the shell material of 1D core-shell structures for energy storage application, such as CuO@Co-Fe LDH [22] and NiO@Co-Fe LDH [36]. However, the fabrication of core-shell 1D heterostructured composite using NiCo<sub>2</sub>O<sub>4</sub> nanowires and Co-Fe LDH nanoflakes has not been explored so far. By combination the high conductive NiCo<sub>2</sub>O<sub>4</sub> nanowire as core with high active Co-Fe LDH as shell, the hierarchical composite is expected to deliver a high performance.

Herein, we synthesized NiCo<sub>2</sub>O<sub>4</sub>@Co-Fe LDH nanowire arrays on nickel foam through simple hydrothermal and calcination methods. The unique core-shell configuration can make use of synergistic effects of two components, provide sufficient electroactive sites and abundance electrolyte diffusion channels. Thus, the as-fabricated composite displays an outstanding electrochemical performance, a high specific capacitance of 1557.5 F g<sup>-1</sup> at 1 A g<sup>-1</sup> and the assembled two-electrode hybrid device NiCo<sub>2</sub>O<sub>4</sub>@Co-Fe LDH//activated carbon (AC) can deliver an energy density of 28.94 Wh kg<sup>-1</sup> at the power density of 950 W kg<sup>-1</sup>.

## 2. Experimental section

### 2.1. Materials preparation

#### 2.1.1. Synthesis of NiCo<sub>2</sub>O<sub>4</sub> nanowire arrays on Ni foam

All the chemical reagents are of analytical grade without further purification. Ni foams were ultra-sonicated in ethanol, 5% HCl solution and deionized water successively, each for 10 min and then dried at 80 °C. Then NiCo<sub>2</sub>O<sub>4</sub> nanowire arrays were fabricated by hydrothermal followed by calcination. 1.19 g CoCl<sub>2</sub>•6H<sub>2</sub>O, 0.59 g NiCl<sub>2</sub>•6H<sub>2</sub>O and 0.53 g urea were dissolved in 50 mL deionized water under magnetic stirring for 30 min at room temperature. Thereafter, the as-obtained homogeneous solution was transferred into an 80 mL Teflon-lined stainless-steel autoclave with pre-treated Ni foam being immersed into the above solution. The autoclave was sealed and then heated at 120 °C for 12 h. After it was cooled down to room temperature, Ni foam coated with pink precursor was taken out and washed with deionized water under ultrasonic treatment for a few minutes. Finally, the precursor was heated at 300 °C for 3 h in air to obtain NiCo<sub>2</sub>O<sub>4</sub> nanowires.

#### 2.1.2. Preparation of NiCo<sub>2</sub>O<sub>4</sub>@Co-Fe LDH core-shell nanowire arrays

The as-prepared NiCo<sub>2</sub>O<sub>4</sub> nanowire arrays were used as scaffold for the further growth of Co-Fe LDH nanoflakes. The Co-Fe LDH was synthesized via another hydrothermal process followed by I<sub>2</sub> oxidation [35]. 0.3807 g CoCl<sub>2</sub>•6H<sub>2</sub>O and 0.0795 g FeCl<sub>2</sub>•4H<sub>2</sub>O were dissolved into 80 mL deionized water which was bubbled by pure nitrogen to eliminate oxygen. Subsequently, 0.2243 g hexamethylenetetramine was added into the solution under a nitrogen atmosphere. Afterwards, the solution was transferred into an 80 mL Teflon-lined stainless-steel autoclave and the as-prepared Ni foam loaded with NiCo<sub>2</sub>O<sub>4</sub> nanowire arrays was soaked into the solution. Then the autoclave was sealed and kept at 90 °C for 3 h. At the same time, 50 mL ethanol solution containing 0.0761 g I<sub>2</sub> was also washed by nitrogen gas for 1 h. After the autoclave cooled down to room temperature, the obtained Ni foam was rapidly taken out and then immersed into above ethanol solution under a nitrogen atmosphere for 2 h at room temperature. Then the Ni foam was collected and washed by deionized water and alcohol repeatedly, and dried at 80 °C.

For comparison, NiCo<sub>2</sub>O<sub>4</sub> nanowires and Co-Fe LDH nanoflakes deposited on Ni foam were simultaneously prepared by the same procedures as-ascribed above. All the mass loading of electrode material was calculated by weighting the Ni foam before and after reaction.

### 2.2. Materials characterization

The crystal structure of as-prepared products was analyzed by X-ray diffractometer (Shimadzu, XRD-6000) using Cu-Kα irradiation (λ = 1.5406 Å) from 10 to 80° with a rate of 3° min<sup>-1</sup>. The chemical composition was investigated by X-ray photoelectron spectroscopy (XPS, Thermo, Escalab 250 Xi). A scanning electron microscope (SEM, Hitachi S-4800) and a transmission electron microscope (TEM, Philips CM200) were used to characterize the structure and morphology of materials. The elemental analysis of NiCo<sub>2</sub>O<sub>4</sub>@Co-Fe LDH was also measured by an electron dispersive X-ray spectrometer (EDS) coupled to the SEM.

### 2.3. Electrochemical measurements for electrode materials

The electrochemical measurements for electrode materials were performed in 2 M KOH aqueous electrolyte by a standard three-electrode system. NiCo<sub>2</sub>O<sub>4</sub>@Co-Fe LDH (≈ 1.5 × 1.5 cm<sup>2</sup>, NiCo<sub>2</sub>O<sub>4</sub> mass ≈ 1.2 mg/cm<sup>2</sup>, Co-Fe LDH mass ≈ 0.5 mg/cm<sup>2</sup>), NiCo<sub>2</sub>O<sub>4</sub> and Co-Fe LDH on Ni foam were directly used as the working electrodes, with Pt foil as the counter electrode and Ag/AgCl electrode as reference electrode. Cyclic voltammograms (CV), galvanostatic charge-discharge (GCD) and electrochemical impedance spectroscopy (EIS) were measured by a CHI660D electrochemical workstation. The cycle life was tested by galvanostatic charge-discharge technique on a LANDCT2001A test system. The specific capacitance (Cs, in F g<sup>-1</sup>) was calculated by the following equation,

$$Cs = I \times t / (m \times \Delta V) \quad (1)$$

wherein I (A), t (s), m (g), ΔV represent the discharge current, discharge time, mass of active material and potential window, respectively.

### 2.4. Electrochemical measurements for hybrid capacitors

A hybrid supercapacitor was assembled by using AC as negative electrode and NiCo<sub>2</sub>O<sub>4</sub>@Co-Fe LDH as positive electrode. The mass of the two electrode materials was balanced to ensure an efficient charge storage according to the equation of Q<sup>+</sup> = Q<sup>-</sup>, where Q<sup>+</sup> and Q<sup>-</sup> are the stored charges of the positive and negative electrodes, respectively. The energy density (E, in Wh kg<sup>-1</sup>) and power density

( $P$ , in  $W\text{ kg}^{-1}$ ) of the hybrid supercapacitor were calculated according to following equations:

$$E = \frac{\int IV(t)dt}{M} \quad (2)$$

$$P = E/t \quad (3)$$

where  $I$  (A),  $V(t)$  (V),  $M$  (g) and  $t$  (s) represent the discharge current, discharge voltage excluding the IR drop, total mass of the active electrode materials and discharge time, respectively.

### 3. Results and discussion

#### 3.1. Chemical and structure characterization

The general synthesis procedure is schematically illustrated in Scheme 1. Initially, through hydrothermal and thermal treatment, highly dense  $\text{NiCo}_2\text{O}_4$  nanowires were grown on the surface of Ni foam. Subsequently, Co-Fe LDH nanoflakes were deposited onto the surface of  $\text{NiCo}_2\text{O}_4$  nanowires by hydrothermal reaction of Co, Fe chloride in alkaline environment, forming a hierarchical core-shell structure. The composite materials on the Ni foam are directly used as electrodes for supercapacitors.

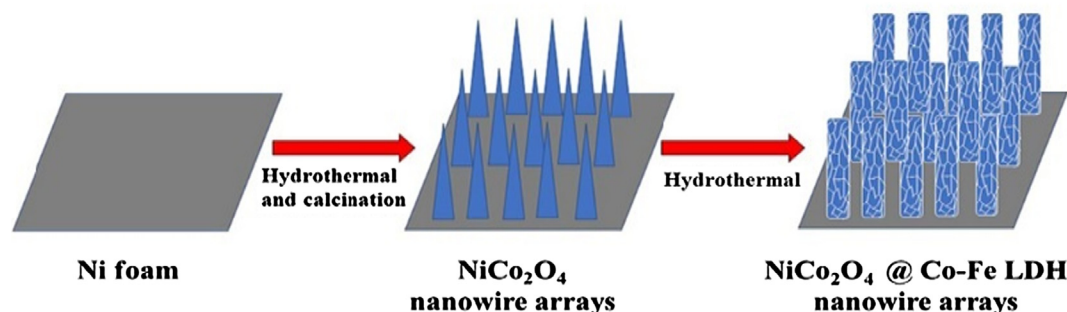
The phase and crystal structure of the as-prepared products were analyzed by X-ray diffraction (XRD). Fig. 1(a) is the XRD patterns of the materials. The strong peaks at  $44.5^\circ$ ,  $51.8^\circ$ ,  $76.3^\circ$  are caused by Ni foam substrate. The diffraction peaks of  $\text{NiCo}_2\text{O}_4$  nanowire arrays can be observed at  $31.1^\circ$ ,  $36.6^\circ$ ,  $44.6^\circ$ ,  $59.1^\circ$  and  $64.9^\circ$  corresponding to the (220), (311), (400), (511), and (440) planes of spinel  $\text{NiCo}_2\text{O}_4$  (JCPDF card No. 20-0781), respectively. Compared with Ni foam, the diffraction peaks of Co-Fe LDH are too weak to be clearly inspected, hence an XRD analysis of Co-Fe LDH from 5 to  $40^\circ$  is further conducted and the result is shown in the inset of Fig. 1(a). The observed peaks at about  $11.6^\circ$ ,  $23.4^\circ$  and  $34.1^\circ$  are well indexed to Co-Fe LDH (PDF No.50-0235). Meanwhile, we can conclude that  $\text{NiCo}_2\text{O}_4$  and Co-Fe LDH were also deposited on the surface of Ni foam from curve *b* and curve *c*, respectively.

X-ray photoelectron spectroscopy (XPS) was performed to further investigate the composition and chemical state of the elements in  $\text{NiCo}_2\text{O}_4$ @Co-Fe LDH, as shown in Fig. 1(b–f). The survey spectrum of  $\text{NiCo}_2\text{O}_4$ @Co-Fe LDH in Fig. 1(b) with peaks of C 1s, O 1s, Ni 2p, Co 2p and Fe 2p indicates the composition of  $\text{NiCo}_2\text{O}_4$ @Co-Fe LDH. The Ni 2p spectrum exhibits two spin-orbit doublets in  $2p_{1/2}$  and  $2p_{3/2}$  electronic configurations at 873.5 eV and 856 eV, respectively (Fig. 1(c)). The peak positions located at 855.9 eV, 856.7 eV, 873.2 eV and 874.4 eV suggest the co-existence of  $\text{Ni}^{2+}$  and  $\text{Ni}^{3+}$  in the sample [37]. In the Co 2p spectrum (Fig. 1(d)), two peaks of  $2p_{1/2}$  and  $2p_{3/2}$  can be observed at the energies of 797.2 eV and 781 eV, respectively. The peaks at 780.8 eV and 796.7 eV are the characteristic of  $\text{Co}^{3+}$ , while the peaks at

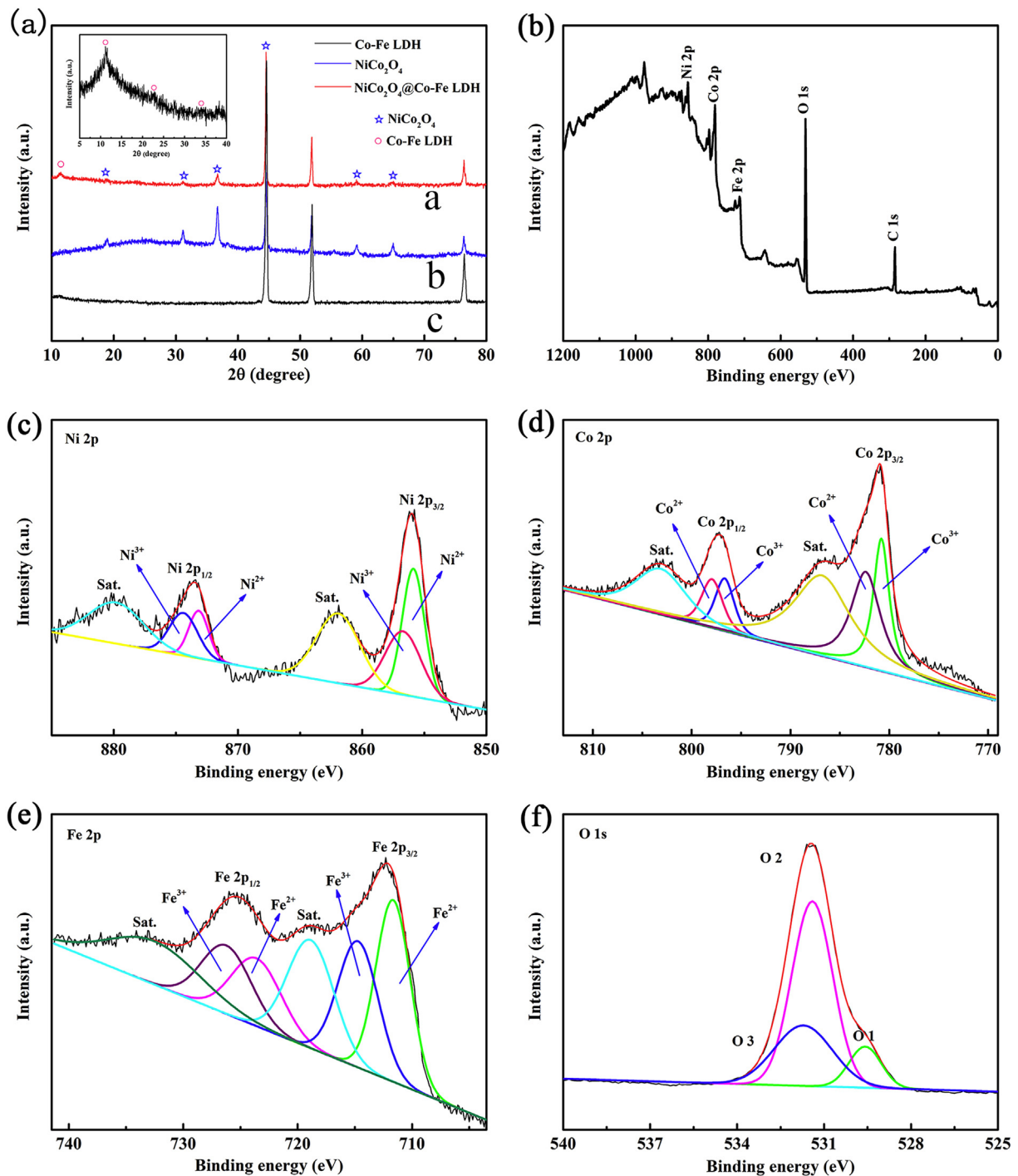
782.4 eV and 797.9 eV are from  $\text{Co}^{2+}$  [38], revealing that different valence states of  $\text{Co}^{2+}$  and  $\text{Co}^{3+}$  exist in  $\text{NiCo}_2\text{O}_4$ @Co-Fe LDH. Fig. 1(e) is the XPS spectrum of Fe 2p. The Fe 2p spectrum is also fitted with two spin-orbit doublets of  $2p_{1/2}$  and  $2p_{3/2}$  at the energies of 712.2 eV and 725.5 eV, respectively. The asymmetry and complication of Fe 2p spectrum indicates the co-existence of  $\text{Fe}^{2+}$  and  $\text{Fe}^{3+}$  [35]. The O 1s spectrum in Fig. 5(f) separates into three peaks, where the peak at 529.6 eV is consistent with absorbed water, the peak of 531.4 eV can be fitted by the presence of hydroxyl group and the peak located at 531.7 eV can be indexed to oxygen species in  $\text{NiCo}_2\text{O}_4$  [34].

Fig. 2(a–d) show the morphologies and microstructures of  $\text{NiCo}_2\text{O}_4$ , Co-Fe LDH and  $\text{NiCo}_2\text{O}_4$ @Co-Fe LDH. Fig. 2(a) reveals that the obtained  $\text{NiCo}_2\text{O}_4$  nanowires are uniformly grown on the surface of the Ni foam substrate with the length of about 5  $\mu\text{m}$ , forming a nanowire array structure completely. In Fig. 2(b), Co-Fe LDH nanoflakes are evenly distributed on Ni foam with the size of several micrometers, from which it can be clearly seen that the nanoflakes closely contact with each other to form a highly porous network film. After hydrothermal deposition,  $\text{NiCo}_2\text{O}_4$  nanowires are entirely wrapped by Co-Fe LDH nanoflakes as shown in Fig. 2(c) and (d) in different magnifications. It can be obviously found that the size of Co-Fe LDH on  $\text{NiCo}_2\text{O}_4$  nanowires is much smaller than that directly grown on the surface of Ni foam in Fig. 2(b), which is beneficial for better electrochemical performance. Fig. 2(d) under a high magnification further reveals that the Co-Fe LDH nanoflakes are interconnected with each other and coated the  $\text{NiCo}_2\text{O}_4$  nanowires intimately, presenting as a highly porous film, which will facilitate the diffusion of electrolyte ions and increase electroactive surface sites. And it can be seen from the sectional images (Fig. S1(a–c)) that  $\text{NiCo}_2\text{O}_4$  nanowires and Co-Fe LDH nanoflakes are both grown on Ni foam substrate closely, hence they can be directly used as electrodes, avoiding the usage of polymer binder and conductive agents. The crystal growth mechanism can be attributed to “oriented attachment” and “self-assembly” processes. The nano-sized  $\text{NiCo}_2\text{O}_4$  core acted as a substrate and then guided the self-assembling growth of Co-Fe LDH on the surface of  $\text{NiCo}_2\text{O}_4$ , which led to a smaller size of Co-Fe LDH compared to the Ni foam due to the higher surface areas of  $\text{NiCo}_2\text{O}_4$  nanowires on Ni foam. Furthermore, the Co-Fe LDH nanoflakes can attach to the surface of  $\text{NiCo}_2\text{O}_4$  to decrease the surface energy [39]. Thus, hierarchical  $\text{NiCo}_2\text{O}_4$ @Co-Fe LDH core-shell nanowire arrays are easily formed.

The microstructure of the obtained materials was further studied by TEM. As shown in Fig. 3(a) and (b),  $\text{NiCo}_2\text{O}_4$  nanowires with diameters about 50–200 nm are composed of a large number of nanoparticles about 5 nm in size. From the HRTEM image in Fig. 3(b), the measured lattice fringes are 0.29 and 0.24 nm, corresponding to the distances of the (220) and (311) planes, respectively, indicating the cubic spinel structure of  $\text{NiCo}_2\text{O}_4$  crystal. Fig. 3(c) shows that the composite is composed of  $\text{NiCo}_2\text{O}_4$  nanowires as core and Co-Fe LDH nanoflakes as shell, from which it



Scheme 1. The illustration of the fabrication process of  $\text{NiCo}_2\text{O}_4$ @Co-Fe LDH nanowire arrays on Ni foam.



**Fig. 1.** (a) XRD patterns of NiCo<sub>2</sub>O<sub>4</sub>, Co-Fe LDH and NiCo<sub>2</sub>O<sub>4</sub>@Co-Fe LDH, XPS spectra of NiCo<sub>2</sub>O<sub>4</sub>@Co-Fe LDH, (b) survey spectrum, (c) Ni 2p, (d) Co 2p, (e) Fe 2p and (f) O 1s.

can be clearly seen that the interconnected nanoflakes are tightly bonded to NiCo<sub>2</sub>O<sub>4</sub> nanowire to form a highly porous hierarchical core-shell heterostructure. The selected area electron diffraction (SEAD) pattern in Fig. 3(d) indicates the multicrystal characteristic of the composite. Several diffraction points from some NiCo<sub>2</sub>O<sub>4</sub> planes are marked in the image. The composition analysis measured by EDS in Fig. S2 shows that the NiCo<sub>2</sub>O<sub>4</sub>@Co-Fe LDH is mainly composed of elements Ni, Co, Fe and O. The atomic percentage in the composite is 12.50%, 19.35% and 5.6% for Ni, Co and Fe, respectively. But the presence of Ni foam substrate may influence the ratio of each element. Fig. 3(e-i) demonstrate the EDS elemen-

tal mappings of NiCo<sub>2</sub>O<sub>4</sub>@Co-Fe LDH nanowire arrays. The uniformly spacial distribution of Ni, Co, Fe and O in the NiCo<sub>2</sub>O<sub>4</sub>@Co-Fe LDH further proves that Co-Fe LDH nanoflakes are homogeneously distributed on the surface of NiCo<sub>2</sub>O<sub>4</sub> nanowires.

### 3.2. Electrochemical performance

To test the electrochemical properties of NiCo<sub>2</sub>O<sub>4</sub> nanowire arrays, NiCo<sub>2</sub>O<sub>4</sub>@Co-Fe LDH core/shell nanowire arrays and Co-Fe

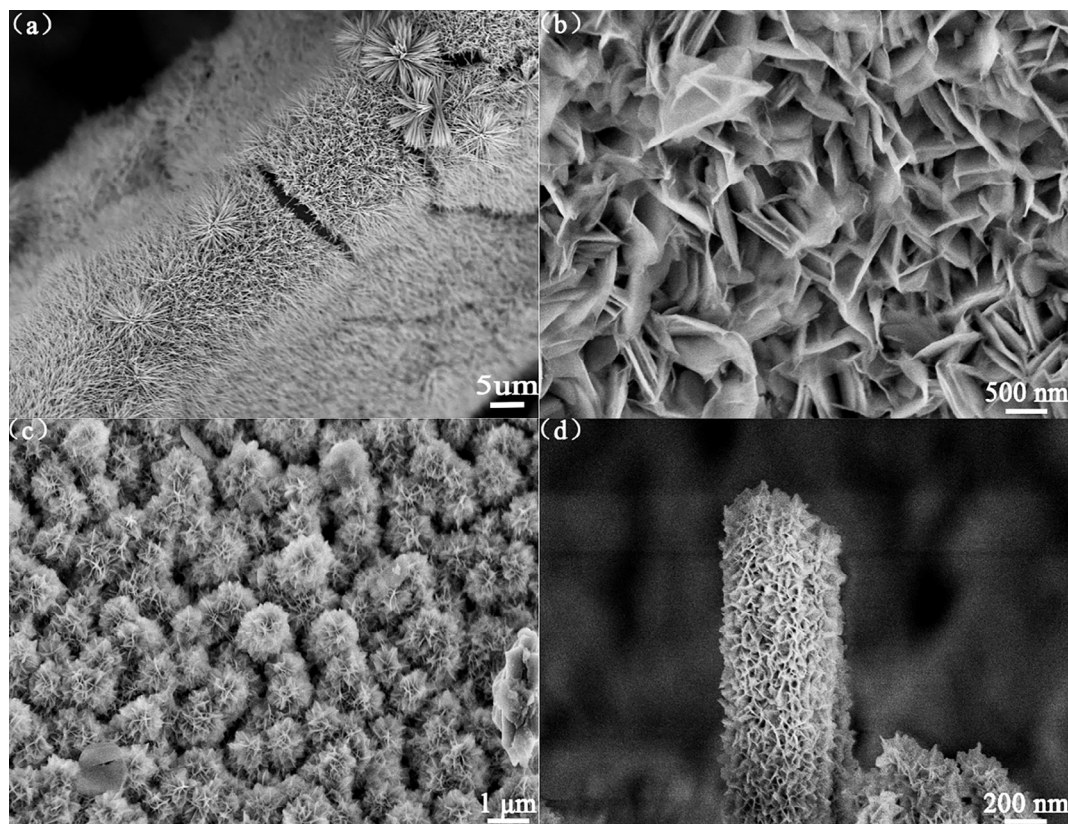
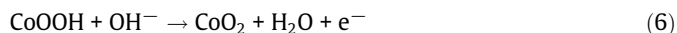
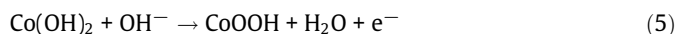


Fig. 2. SEM images of (a) NiCo<sub>2</sub>O<sub>4</sub> nanowire arrays on Ni foam, (b) Co-Fe LDH nanoflakes on Ni foam, (c-d) NiCo<sub>2</sub>O<sub>4</sub>@Co-Fe LDH nanowire arrays on Ni foam.

LDH on Ni foam, CV, GCD and EIS measurements in a three-electrode system in 2 M KOH were conducted.

Fig. 4(a) shows the CV curves of NiCo<sub>2</sub>O<sub>4</sub>@Co-Fe LDH electrode at different scan rates within a potential range from 0 to 0.5 V. The CV curves of NiCo<sub>2</sub>O<sub>4</sub> and Co-Fe LDH are shown in Fig. S3(a) and (b), respectively. The obvious redox peaks can be attributed to the surface Faradaic redox reactions. The position of the redox peaks shifts with the increasing scan rates, this serious electrochemical polarization phenomenon is caused by the low electrical conductivity of the electrode material, which will limit charge transfer and ion transport at high scan rate. Fig. 4(b) displays the CV curves of NiCo<sub>2</sub>O<sub>4</sub> nanowire arrays, Co-Fe LDH and NiCo<sub>2</sub>O<sub>4</sub>@Co-Fe LDH nanowire arrays at 5 mV s<sup>-1</sup> for a comparison. The 0.16 V of anodic peak for NiCo<sub>2</sub>O<sub>4</sub>, 0.17 V for NiCo<sub>2</sub>O<sub>4</sub>@Co-Fe LDH and 0.24 V for Co-Fe LDH are clearly observed, and the cathodic peaks at 0.45 V, 0.45 V and 0.39 V are corresponded to their reverse process, respectively. The surface Faradaic redox reactions can be described as Eqs. (4–6) [40,41]. Furthermore, the CV integrated area of NiCo<sub>2</sub>O<sub>4</sub>@Co-Fe LDH is larger than those of NiCo<sub>2</sub>O<sub>4</sub> and Co-Fe LDH, indicating its better electrochemical performance.



The GCD curves of NiCo<sub>2</sub>O<sub>4</sub>@Co-Fe LDH nanowire arrays at different current densities are shown in Fig. 4(c) and the GCD curves of NiCo<sub>2</sub>O<sub>4</sub> and Co-Fe LDH are shown in Fig. S3(c) and (d), respectively. The apparent voltage plateaus demonstrate the existence of Faradic redox reactions, and they match well with the redox peaks in the CV curves. The good symmetry of GCD curves indicates that

the sample has a high coulombic efficiency. Fig. 4(d) displays the comparison of GCD curves of NiCo<sub>2</sub>O<sub>4</sub> nanowire arrays, Co-Fe LDH and NiCo<sub>2</sub>O<sub>4</sub>@Co-Fe LDH nanowire arrays at the same current density of 1 A g<sup>-1</sup>. Evidently, NiCo<sub>2</sub>O<sub>4</sub>@Co-Fe LDH electrode (623 s) shows much longer discharge time than both NiCo<sub>2</sub>O<sub>4</sub> electrode (393 s) and Co-Fe LDH (182 s), revealing that the NiCo<sub>2</sub>O<sub>4</sub>@Co-Fe LDH electrode possesses the highest specific capacitance. Then, the specific capacitance of three materials are calculated from the GCD curves according to Eq. (1) and the values are shown in Fig. 4(e). The specific capacitance for NiCo<sub>2</sub>O<sub>4</sub>@Co-Fe LDH is 1557.5, 1362.5, 985, 660 and 550 F g<sup>-1</sup> at the current density of 1, 2, 5, 8, 10 A g<sup>-1</sup>, respectively. While the values for NiCo<sub>2</sub>O<sub>4</sub> are 982.5, 931.5, 798.75, 740 and 662.5 F g<sup>-1</sup> under the same conditions. Meanwhile, the specific capacitance of Co-Fe LDH is 455, 361.5, 232.5, 156, 122.5 F g<sup>-1</sup> under the same above current densities. The electrochemical performance of Co-Fe LDH is worse than the other two electrodes, which is well consistent with the result of CV curves. Furthermore, it can be seen that NiCo<sub>2</sub>O<sub>4</sub>@Co-Fe LDH nanowire arrays possess a much higher capacitance than NiCo<sub>2</sub>O<sub>4</sub> nanowire arrays at low current densities, whereas the result is converse at high current densities, indicating the inferior rate capability of the composite. The result of its higher capacitance can be attributed to the fact that the “shell” Co-Fe LDH increases electroactive surface sites for redox reaction and the porous structure provides abundant electrolyte diffusion channels. However, the combination of Co-Fe LDH on highly conductive NiCo<sub>2</sub>O<sub>4</sub> nanowire decreases the total conductivity and causes a higher resistance than pure NiCo<sub>2</sub>O<sub>4</sub> nanowires, which will limit the diffusion of ions and electrons at high current densities. As a consequence, the composite displays a worse rate capability than NiCo<sub>2</sub>O<sub>4</sub> nanowires under high current density.

To further research the interfacial kinetics of electrode materials, EIS is measured and the Nyquist plots are shown in Fig. 4(f).

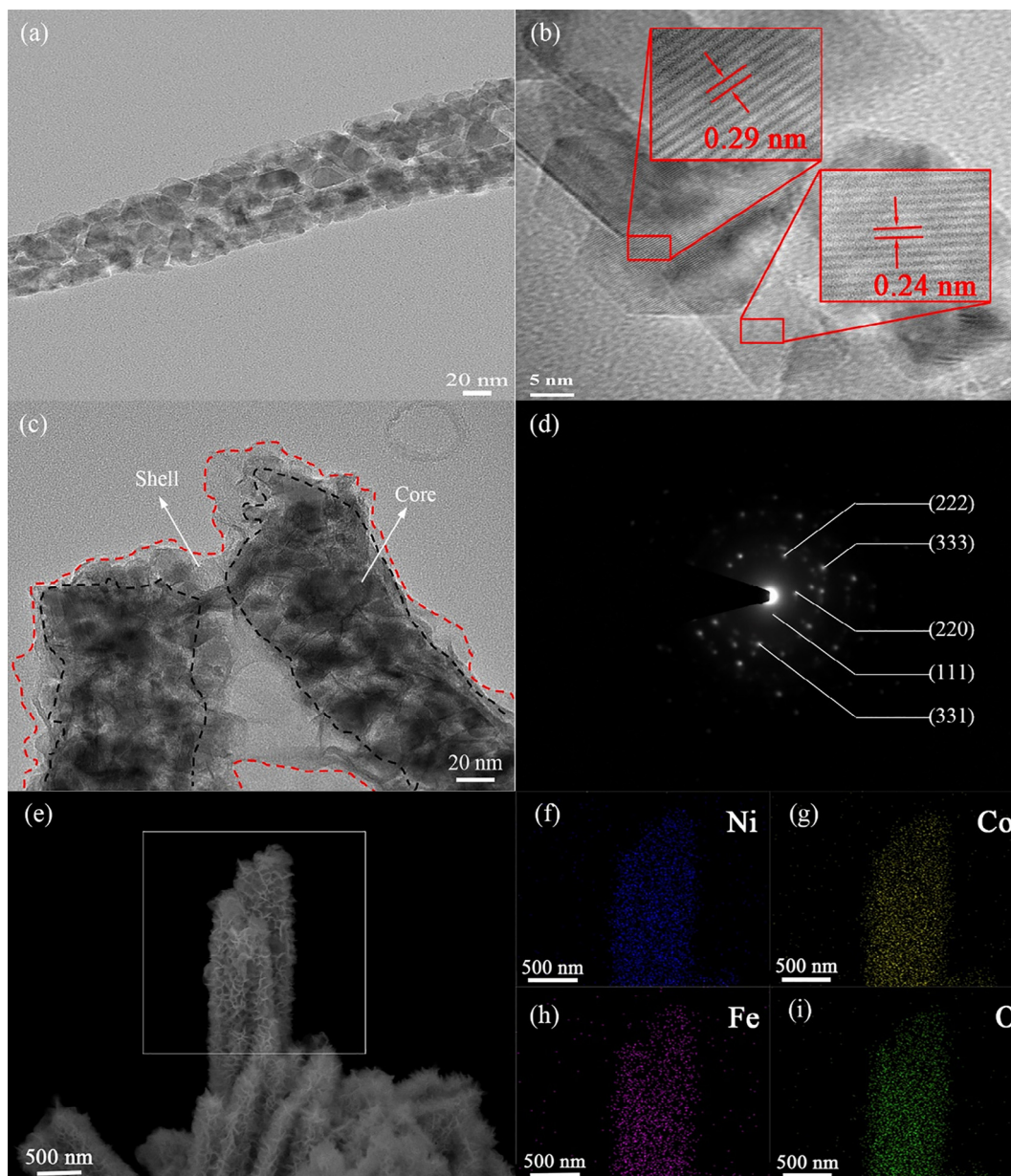


**Fig. 3.** TEM images of (a and b)  $\text{NiCo}_2\text{O}_4$  nanowire and (c)  $\text{NiCo}_2\text{O}_4@$ Co-Fe LDH, (d) selected area electron diffraction of the  $\text{NiCo}_2\text{O}_4@$ Co-Fe LDH, (e) SEM image of the selected-area for elemental mapping analysis, (f–i) elemental mappings of Ni, Co, Fe and O.

Each EIS plot can be divided into two parts, a straight sloping line in low-frequency area and a small semi-circle in high-frequency region [42]. The curves are all simulated in Fig. S4(a–c), and their equivalent circuit is shown in the inset of Fig. 4(f). At low frequency, the slope of the curves represents the Warburg impedance (W1), which means the diffusion resistance of the electrolyte. It can be seen that  $\text{NiCo}_2\text{O}_4$  nanowire arrays has the most ideal straight line along the imaginary axis, showing its lowest diffusion resistance. The diffusion resistance of  $\text{NiCo}_2\text{O}_4@$ Co-Fe LDH is larger than  $\text{NiCo}_2\text{O}_4$ , which can be explained by the fact that the surface of  $\text{NiCo}_2\text{O}_4$  nanowires are wrapped by Co-Fe LDH, whereas the poor conductivity of Co-Fe LDH will limit the diffusion of electrolyte ions. At high frequency, the intercept on the real axis displays the equivalent series resistance (R1) and the semicircle indicates the charge-transfer resistance (R2). As shown in the inset,  $\text{NiCo}_2\text{O}_4@$ Co-Fe LDH has a smaller R1 value (0.42  $\Omega$ ) than  $\text{NiCo}_2\text{O}_4$  (0.55  $\Omega$ ) and Co-Fe LDH (0.81  $\Omega$ ), suggesting its better electronic

conductivity. For charge transfer resistance, the calculated R2 values for  $\text{NiCo}_2\text{O}_4@$ Co-Fe LDH,  $\text{NiCo}_2\text{O}_4$  and Co-Fe LDH are 0.36, 0.20 and 2.15  $\Omega$ , respectively. The charge transfer resistance of Co-Fe LDH is much higher than the others. And the Co-Fe LDH nanoflakes on the surface of  $\text{NiCo}_2\text{O}_4$  nanowires somehow decrease the conductivity of the composite material. The repeated charge-discharge measurements for 5000 cycles were conducted at 5 A  $\text{g}^{-1}$  to test the cycling stability of the three electrode materials, as shown in Fig. S4(d). The specific capacitance retention for  $\text{NiCo}_2\text{O}_4@$ Co-Fe LDH,  $\text{NiCo}_2\text{O}_4$  and Co-Fe LDH is 59.1%, 77.8% and 61.5%, respectively.  $\text{NiCo}_2\text{O}_4$  shows the best cycling stability, whereas both  $\text{NiCo}_2\text{O}_4@$ Co-Fe LDH and Co-Fe LDH display a comparable low stability. It can be ascribed to the structural change of Co-Fe hydroxides during the long-time Faradic reaction [35].

To reach a high energy density and power density, the design of hybrid capacitors has received much attention. Unlike traditional supercapacitors, hybrid capacitors consist of two different elec-

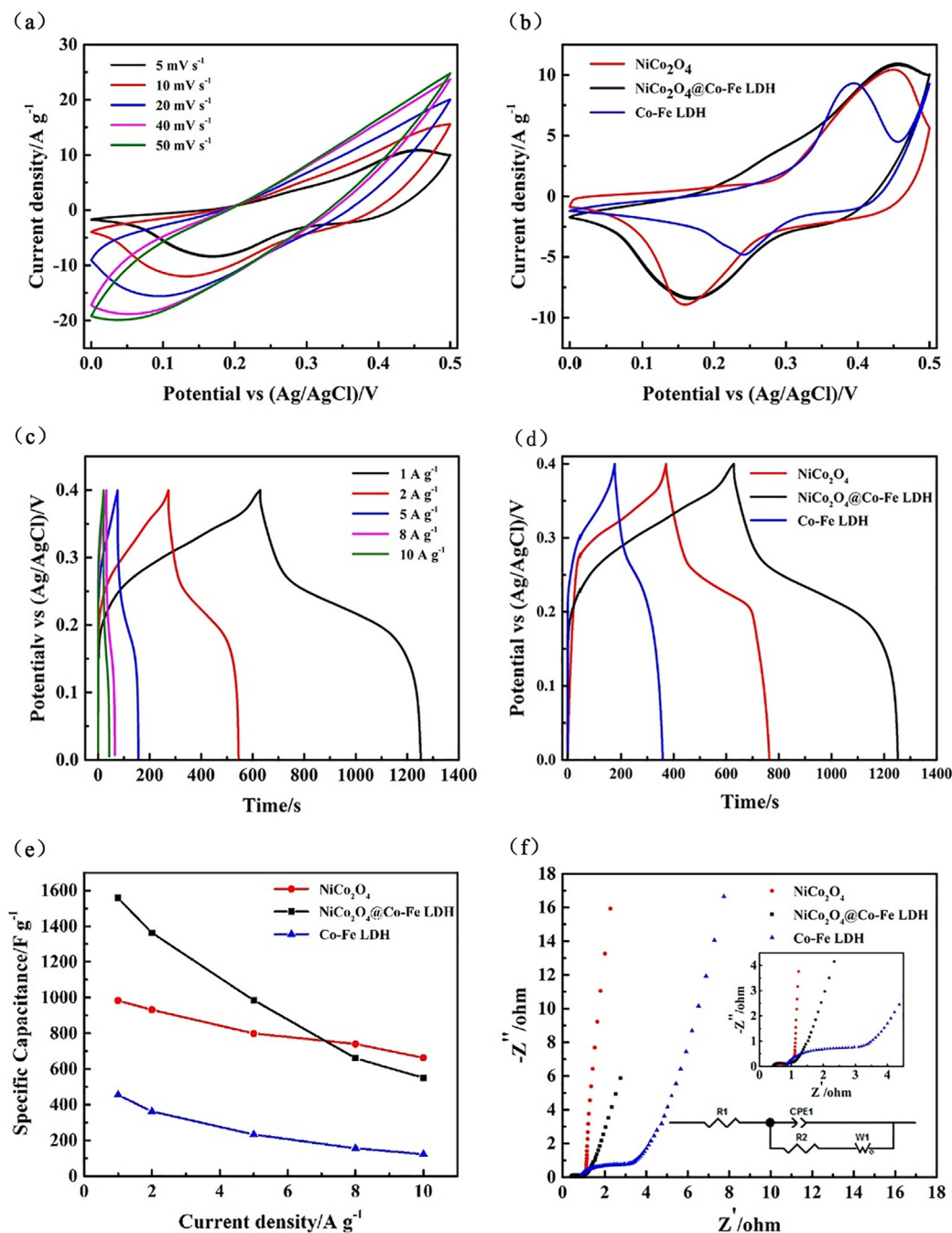


**Fig. 4.** Electrochemical characterization of the materials in 2 M KOH, (a) CV curves of NiCo<sub>2</sub>O<sub>4</sub>@Co-Fe LDH at various scan rates, (b) CV curves of the three materials at the scan rate of 5 mV s<sup>-1</sup>, (c) GCD curves of NiCo<sub>2</sub>O<sub>4</sub>@Co-Fe LDH at different current densities, (d) GCD curves of the three materials at the current density of 1 A g<sup>-1</sup>, (e) specific capacitance at various current densities and (f) Nyquist plots for the different materials.

trodes, i.e., a capacitor-type electrode as a power source and a battery-type Faradaic electrode as an energy source [43]. In order to explore the electrochemical performance of NiCo<sub>2</sub>O<sub>4</sub>@Co-Fe LDH for practical application, a hybrid capacitor was assembled by using it as positive electrode and AC (18.48 mg) as negative electrode in 2 M KOH aqueous electrolyte. Fig. 5(a) shows the CV curves of an AC electrode and NiCo<sub>2</sub>O<sub>4</sub>@Co-Fe LDH electrode at the scan rate of 5 mV s<sup>-1</sup> in a three-electrode system. The nearly rectangle shape of the CV curve for AC proves its typical EDLC behavior. The CV curves at different scan rates of the hybrid capacitor are exhibited in Fig. 5(b), which reveal a dual energy storage mechanism of the energy storage device. Fig. 5(c) displays the

GCD curves of the hybrid capacitor at various current densities. The symmetric curves demonstrate the good coulombic efficiency of the hybrid capacitor, and the slight voltage plateaus indicate the existence of Faradaic reaction, corresponding well with the CV curves. The specific capacitance based on the total mass of two electrodes calculated by Eq. (1) are 64.76, 53.88, 44.65, 40, 39.71 F g<sup>-1</sup> at 1, 2, 3, 4 and 5 A g<sup>-1</sup>, respectively, as shown in the inset of Fig. 5(d). The specific capacitance at 5 A g<sup>-1</sup> can still remain 61.3% of that at 1 A g<sup>-1</sup>, indicating a moderate rate capability. The energy and power densities of the hybrid capacitor are calculated by Eq. (2) and Eq. (3), respectively, as presented as a Ragone plot in Fig. 5(d). The hybrid capacitor of NiCo<sub>2</sub>O<sub>4</sub>@Co-Fe LDH//AC shows

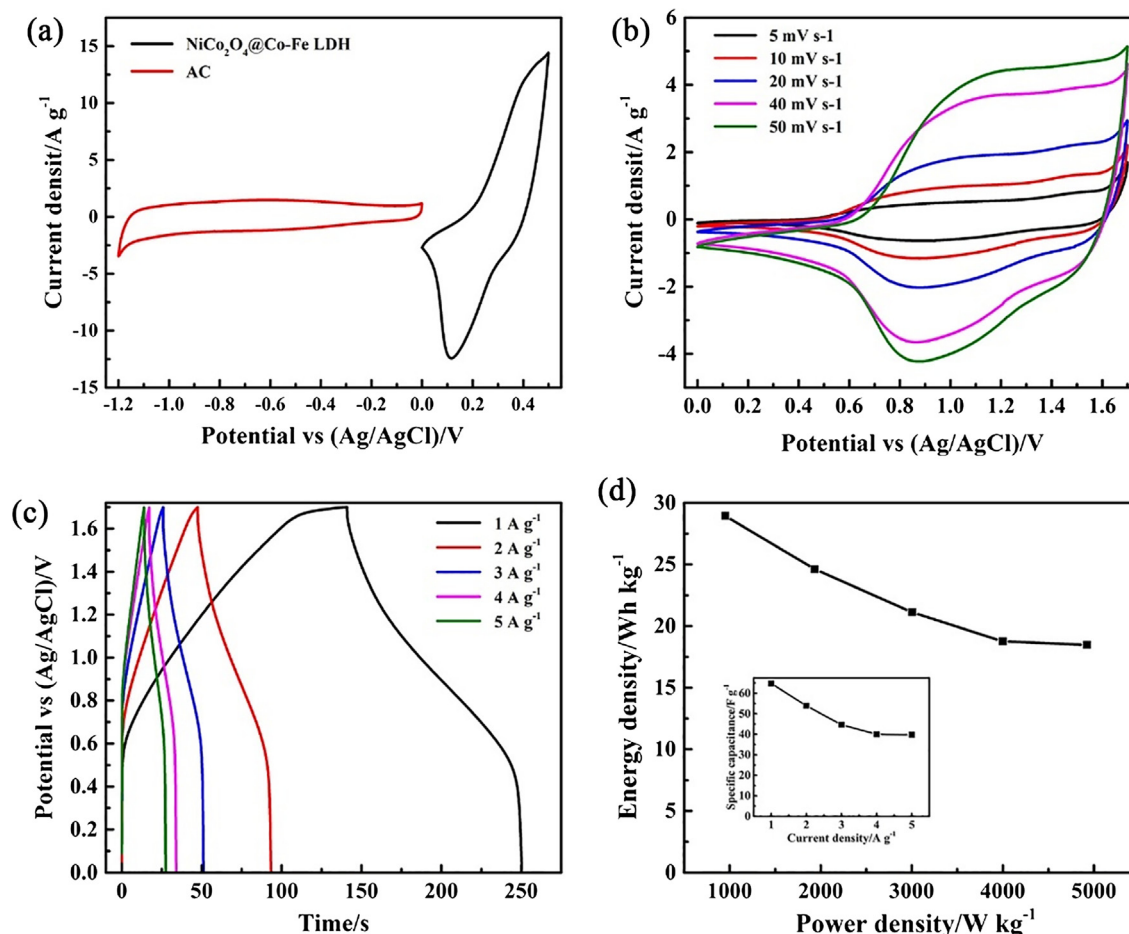


**Fig. 5.** (a) CV curves of NiCo<sub>2</sub>O<sub>4</sub>@Co-Fe LDH and AC at the scan rate of 5 mV s<sup>-1</sup>, (b) CV curves of the hybrid capacitor at various scan rates, (c) GCD curves of the assembled hybrid capacitor at different current densities, (d) Ragone plot of the hybrid capacitor based on NiCo<sub>2</sub>O<sub>4</sub>@Co-Fe LDH (inset displaying the specific capacitance at different current densities).

an energy density of 28.94 Wh kg<sup>-1</sup> at the power density of 950 W kg<sup>-1</sup> and maintains 18.47 Wh kg<sup>-1</sup> at the power density of 4925 W kg<sup>-1</sup>. Compared with previously reported hybrid capacitors, such as NiO@Co-Fe LDH (22 Wh kg<sup>-1</sup>) [36] and NiCo<sub>2</sub>O<sub>4</sub>@NiMoO<sub>4</sub> (21.7 Wh kg<sup>-1</sup>) [44], the NiCo<sub>2</sub>O<sub>4</sub>@Co-Fe LDH//AC capacitor in this work shows a higher energy density. The cycling stability of the device is also examined and shown in Fig. S5. 76.9% retention of the initial specific capacitance after 5000 cycles at 2 A g<sup>-1</sup> reveals the outstanding cycling stability of the hybrid supercapacitor. Therefore, the assembled hybrid capacitor has great potential in practical energy storage.

#### 4. Conclusion

In conclusion, hierarchical NiCo<sub>2</sub>O<sub>4</sub>@Co-Fe LDH core-shell nanowire arrays are successfully synthesized by a facile procedure. This novel core-shell structured electrode material offers plenty of advantages as follows: (1) the material deposited on Ni foam can be directly used as electrode, avoiding the usage of polymer binder and conductive agents. (2) The firstly-grown NiCo<sub>2</sub>O<sub>4</sub> nanowire arrays serve as backbone for the subsequent growth of Co-Fe LDH nanoflakes, providing more electroactive surface sites. (3) The reasonable combination of NiCo<sub>2</sub>O<sub>4</sub> and Co-Fe LDH can make full use of potential synergistic effects. Consequently, the fabricated NiCo<sub>2</sub>O<sub>4</sub>@Co-Fe LDH nanowire arrays displayed an outstanding electrochemical performance, with a high specific capacitance of 1557.5 F g<sup>-1</sup> at 1 A g<sup>-1</sup> and the assembled two-electrode hybrid

device NiCo<sub>2</sub>O<sub>4</sub>@Co-Fe LDH//activated carbon could deliver an energy density of 28.94 Wh kg<sup>-1</sup> at the power density of 950 W kg<sup>-1</sup>.

#### Acknowledgments

This work was supported by the Natural Science Foundation of China (No. 81472961) and Zhejiang Provincial Natural Science Foundation of China (No. LY18E020003).

#### Appendix A. Supplementary material

Supplementary data associated with this article can be found, in the online version, at <https://doi.org/10.1016/j.apsusc.2018.04.254>.

#### References

- [1] X. Lu, C. Wang, F. Favier, N. Pinna, Electrospun nanomaterials for supercapacitor electrodes: designed architectures and electrochemical performance, *Adv. Energy Mater.* 7 (2017) 1601301.
- [2] P. Simon, Y. Gogotsi, Materials for electrochemical capacitors, *Nat. Mater.* 7 (2008) 845.
- [3] Y. Wang, Y. Song, Y. Xia, Electrochemical capacitors: mechanism, materials, systems, characterization and applications, *Chem. Soc. Rev.* 45 (2016) 5925–5950.
- [4] Q. Shou, J. Cheng, L. Zhang, B.J. Nelson, X. Zhang, Synthesis and characterization of a nanocomposite of goethite nanorods and reduced graphene oxide for electrochemical capacitors, *J. Solid State Chem.* 185 (2012) 191–197.
- [5] L.L. Zhang, X.S. Zhao, Carbon-based materials as supercapacitor electrodes, *Chem. Soc. Rev.* 38 (2009) 2520–2531.

- [6] C. Zhong, Y. Deng, W. Hu, J. Qiao, L. Zhang, J. Zhang, A review of electrolyte materials and compositions for electrochemical supercapacitors, *Chem. Soc. Rev.* 44 (2015) 7484–7539.
- [7] G. Wang, L. Zhang, J. Zhang, A review of electrode materials for electrochemical supercapacitors, *Chem. Soc. Rev.* 41 (2012) 797–828.
- [8] Q. Meng, K. Cai, Y. Chen, L. Chen, Research progress on conducting polymer based supercapacitor electrode materials, *Nano Energy* 36 (2017) 268–285.
- [9] W. Deng, X. Ji, Q. Chen, C.E. Banks, Electrochemical capacitors utilising transition metal oxides: an update of recent developments, *Rsc Adv.* 1 (2011) 1171–1178.
- [10] X. Li, D. Du, Y. Zhang, W. Xing, Q. Xue, Z. Yan, Layered double hydroxides toward high-performance supercapacitors, *J. Mater. Chem. A* 5 (2017) 15460–15485.
- [11] Z. Lu, Q. Yang, W. Zhu, Z. Chang, J. Liu, X. Sun, D.G. Evans, X. Duan, Hierarchical  $\text{Co}_3\text{O}_4$ @Ni-Co-O supercapacitor electrodes with ultrahigh specific capacitance per area, *Nano Res.* 5 (2012) 369–378.
- [12] G. Zhang, T. Wang, X. Yu, H. Zhang, H. Duan, B. Lu, Nanoforest of hierarchical  $\text{Co}_3\text{O}_4$ @ $\text{NiCo}_2\text{O}_4$  nanowire arrays for high-performance supercapacitors, *Nano Energy* 2 (2013) 586–594.
- [13] X.F. Lu, X.Y. Chen, W. Zhou, Y.X. Tong, G.R. Li,  $\alpha\text{-Fe}_2\text{O}_3$ @PANI Core-Shell Nanowire Arrays as Negative Electrodes for Asymmetric Supercapacitors, *ACS Appl. Mater. Interfaces* 7 (2015) 14843–14850.
- [14] G. Zhang, X. Xiao, B. Li, P. Gu, H. Xue, H. Pang, Transition metal oxides with one-dimensional/one-dimensional-analogue nanostructures for advanced supercapacitors, *J. Mater. Chem. A* 5 (2017) 8155–8186.
- [15] L.B. Jiang, X.Z. Yuan, J. Liang, J. Zhang, H. Wang, G.-M. Zeng, Nanostructured core-shell electrode materials for electrochemical capacitors, *J. Power Sources* 331 (2016) 408–425.
- [16] Z. Yu, L. Tetaud, L. Zhai, J. Thomas, Supercapacitor electrode materials: nanostructures from 0 to 3 dimensions, *Energy Environ. Sci.* 8 (2015) 702–730.
- [17] H.L.Y.L. Wang, X.X. Liu, R. Zeng, M. Li, Y.H. Huang, X.L. Hu, Constructing Hierarchical Tectorumlike  $\alpha\text{-Fe}_2\text{O}_3$ /PPy Nanoarrays on Carbon Cloth for Solid-state Asymmetric Supercapacitors, *Angew. Chem. Int. Edit.* 129 (2017) 1125–1130.
- [18] J. Liu, J. Jiang, C. Cheng, H. Li, J. Zhang, H. Gong, H.J. Fan,  $\text{Co}_3\text{O}_4$  Nanowire@ $\text{MnO}_2$  ultrathin nanosheet core/shell arrays: a new class of high-performance pseudocapacitive materials, *Adv. Mater.* 23 (2011) 2076–2081.
- [19] X. Wu, L. Meng, Q. Wang, W. Zhang, Y. Wang, A flexible asymmetric fibered-supercapacitor based on unique  $\text{Co}_3\text{O}_4$ @PPy core-shell nanorod arrays electrode, *Chem. Eng. J.* 327 (2017) 193–201.
- [20] C. Guan, J. Liu, C. Cheng, H. Li, X. Li, W. Zhou, H. Zhang, H.J. Fan, Hybrid structure of cobalt monoxide nanowire @ nickel hydroxidenitrate nanoflake aligned on nickel foam for high-rate supercapacitor, *Energy Environ. Sci.* 4 (2011) 4496.
- [21] D. Cai, H. Huang, D. Wang, B. Liu, L. Wang, Y. Liu, Q. Li, T. Wang, High-Performance Supercapacitor Electrode Based on the Unique  $\text{ZnO}/\text{Co}_3\text{O}_4$  Core/Shell Heterostructures on Nickel Foam, *ACS Appl. Mater. Interfaces* 6 (2014) 15905.
- [22] Z. Li, M. Shao, L. Zhou, R. Zhang, C. Zhang, J. Han, M. Wei, D.G. Evans, X. Duan, A flexible all-solid-state micro-supercapacitor based on hierarchical  $\text{CuO}/\text{layered double hydroxide}$  core-shell nanoarrays, *Nano Energy* 20 (2016) 294–304.
- [23] Y.F. Yuan, J.X. Lin, D. Zhang, S.M. Yin, Y.L. Zhao, J.L. Yang, Y.B. Chen, S.Y. Guo, Freestanding hierarchical  $\text{NiO}/\text{MnO}_2$  core/shell nanocomposite arrays for high-performance electrochemical energy storage, *Electrochim. Acta.* 227 (2017) 303–309.
- [24] S. Liu, L. Hu, X. Xu, A.A. Al-Ghamdi, X. Fang, Nickel Cobaltite Nanostructures for Photoelectric and Catalytic Applications, *Small.* 11 (2015) 4267–4283.
- [25] L. Wang, X. Jiao, P. Liu, Y. Ouyang, X. Xia, W. Lei, Q. Hao, Self-template synthesis of yolk-shelled  $\text{NiCo}_2\text{O}_4$  spheres for enhanced hybrid supercapacitors, *Appl. Surf. Sci.* 427 (2018) 174–181.
- [26] L. Yu, G. Zhang, C. Yuan, X.W. Lou, Hierarchical  $\text{NiCo}_2\text{O}_4$ @ $\text{MnO}_2$  core-shell heterostructured nanowire arrays on Ni foam as high-performance supercapacitor electrodes, *Chem Commun (Camb).* 49 (2013) 137–139.
- [27] S. Chen, G. Yang, Y. Jia, H. Zheng, Three-dimensional  $\text{NiCo}_2\text{O}_4$ @ $\text{NiWO}_4$  core-shell nanowire arrays for high performance supercapacitors, *J. Mater. Chem. A* 5 (2017) 1028–1034.
- [28] J. Cheng, J. Zhang, F. Liu, Recent development of metal hydroxides as electrode material of electrochemical capacitors, *RSC Adv.* 4 (2014) 38893–38917.
- [29] I. Lee, G.H. Jeong, S. An, S.-W. Kim, S. Yoon, Facile synthesis of 3D MnNi-layered double hydroxides (LDH)/graphene composites from directly graphites for pseudocapacitor and their electrochemical analysis, *Appl. Surf. Sci.* 429 (2018) 196–202.
- [30] M. Li, J.P. Cheng, J. Wang, F. Liu, X.B. Zhang, The growth of nickel-manganese and cobalt-manganese layered double hydroxides on reduced graphene oxide for supercapacitor, *Electrochim. Acta.* 206 (2016) 108–115.
- [31] M. Li, J.P. Cheng, F. Liu, X.B. Zhang, 3D-architected nickel-cobalt-manganese layered double hydroxide/reduced graphene oxide composite for high-performance supercapacitor, *Chem. Phys. Lett.* 640 (2015) 5–10.
- [32] F. Ning, M. Shao, C. Zhang, S. Xu, M. Wei, X. Duan,  $\text{Co}_3\text{O}_4$ @layered double hydroxide core/shell hierarchical nanowire arrays for enhanced supercapacitive performance, *Nano Energy* 7 (2014) 134–142.
- [33] J. Han, Y. Dou, J. Zhao, M. Wei, D.G. Evans, X. Duan, Flexible CoAl LDH@PEDOT Core/Shell Nanoplatelet Array for High-Performance Energy Storage, *Small* 9 (2013) 98–106.
- [34] X. He, Q. Liu, J. Liu, R. Li, H. Zhang, R. Chen, J. Wang, Hierarchical  $\text{NiCo}_2\text{O}_4$ @ $\text{NiCoAl}$ -layered double hydroxide core/shell nanoforest arrays as advanced electrodes for high-performance asymmetric supercapacitors, *J. Alloys Compd.* 724 (2017) 130–138.
- [35] K. Ma, J.P. Cheng, J. Zhang, M. Li, F. Liu, X. Zhang, Dependence of Co/Fe ratios in Co-Fe layered double hydroxides on the structure and capacitive properties, *Electrochim. Acta* 198 (2016) 231–240.
- [36] K.Y. Ma, F. Liu, M. Zhang, X. Zhang, J.P. Cheng, Core/shell microrod arrays of  $\text{NiO}/\text{Co-Fe}$  layered double hydroxides deposited on nickel foam for energy storage and conversion, *Electrochim. Acta* 225 (2017) 425–434.
- [37] D.U. Lee, B.J. Kim, Z. Chen, One-pot synthesis of a mesoporous  $\text{NiCo}_2\text{O}_4$  nanoplatelet and graphene hybrid and its oxygen reduction and evolution activities as an efficient bi-functional electrocatalyst, *J. Mater. Chem. A* 1 (2013) 4754.
- [38] D. Xia, H. Chen, J. Jiang, L. Zhang, Y. Zhao, D. Guo, J. Yu, Facilely synthesized  $\alpha$  phase nickel-cobalt bimetallic hydroxides: Tuning the composition for high pseudocapacitance, *Electrochim. Acta* 156 (2015) 108–114.
- [39] L.Q. Mai, F. Yang, Y.L. Zhao, X. Xu, L. Xu, Y.Z. Luo, Hierarchical  $\text{MnMoO}_4/\text{CoMoO}_4$  heterostructured nanowires with enhanced supercapacitor performance, *Nat Commun* 2 (2011) 381.
- [40] W. Zhou, D. Kong, X. Jia, C. Ding, C. Cheng, G. Wen,  $\text{NiCo}_2\text{O}_4$  nanosheet supported hierarchical core-shell arrays for high-performance supercapacitors, *J. Mater. Chem. A* 2 (2014) 6310.
- [41] X. Wu, L. Jiang, C. Long, T. Wei, Z. Fan, Dual support system ensuring porous Co-Al hydroxide nanosheets with ultrahigh rate performance and high energy density for supercapacitors, *Adv. Funct. Mater.* 25 (2015) 1648–1655.
- [42] J. Wang, K.Y. Ma, J. Zhang, F. Liu, J.P. Cheng, Template-free synthesis of hierarchical hollow  $\text{NiS}_x$  microspheres for supercapacitor, *J. Colloid Interf. Sci.* 507 (2017) 290–299.
- [43] N. Choudhary, C. Li, J. Moore, N. Nagaiah, L. Zhai, Y. Jung, J. Thomas, Asymmetric supercapacitor electrodes and devices, *Adv Mater* 29 (2017) 1605336.
- [44] D. Cheng, Y. Yang, J. Xie, C. Fang, G. Zhang, J. Xiong, Hierarchical  $\text{NiCo}_2\text{O}_4$ @ $\text{NiMoO}_4$  core-shell hybrid nanowire/nanosheet arrays for high-performance pseudocapacitors, *J. Mater. Chem. A* 3 (2015) 14348–14357.